



## Potassium diffusion in melilite: Experimental studies and constraints on the thermal history and size of planetesimals hosting CAIs

Motoo ITO and Jibamitra GANGULY\*

Department of Geosciences, University of Arizona, Tucson, Arizona 85721, USA

\*Corresponding author. E-mail: [ganguly@geo.arizona.edu](mailto:ganguly@geo.arizona.edu)

(Received 24 May 2004; revision accepted 27 September 2004)

**Abstract**—Among the calcium-aluminum-rich inclusions (CAIs), excess  $^{41}\text{K}$  ( $^{41}\text{K}^*$ ), which was produced by the decay of the short-lived radionuclide  $^{41}\text{Ca}$  ( $t_{1/2} = 0.1$  Myr), has so far been detected in fassaite and in two grains of melilites. These observations could be used to provide important constraints on the thermal history and size of the planetesimals into which the CAIs were incorporated, provided the diffusion kinetic properties of K in these minerals are known. Thus, we have experimentally determined K diffusion kinetics in the melilite end-members, åkermanite and gehlenite, as a function of temperature (900–1200 °C) and crystallographic orientation at 1 bar pressure. The closure temperature of K diffusion in melilite,  $T_c(\text{K:mel})$ , for the observed grain size of melilite in the CAIs and cooling rate of 10–100 °C/Myr, as calculated from our diffusion data, is much higher than that of Mg in anorthite. The latter was calculated from the available Mg diffusion data in anorthite. Assuming that the planetesimals were heated by the decay of  $^{26}\text{Al}$  and  $^{60}\text{Fe}$ , we have calculated the size of a planetesimal as a function of the accretion time  $t_f$  such that the peak temperature at a specified radial distance  $r_c$  equals  $T_c(\text{K:mel})$ . The ratio  $(r_c/R)^3$  defines the planetesimal volume fraction within which  $^{41}\text{K}^*$  in melilite grains would be at least partly disturbed, if these were randomly distributed within a planetesimal. A similar calculation was also carried out to define  $R$  versus  $t_f$  relation such that  $^{26}\text{Mg}^*$  was lost from ~50% of randomly distributed anorthite grains, as seems to be suggested by the observational data. These calculations suggest that ~60% of melilite grains should retain  $^{41}\text{K}^*$  if ~50% of anorthite grains had retained  $^{26}\text{Mg}^*$ . Assuming that  $t_f$  was not smaller than the time of chondrule formation, our calculations yield minimum planetesimal radius of ~20–30 km, depending on the choice of planetesimal surface temperature and initial abundance of the heat producing isotope  $^{60}\text{Fe}$ .

### INTRODUCTION

The thermal history, formation time, and size of the planetesimals that accreted during the very early history of the solar system have been subjects of considerable interest in the field of planetary science (e.g., LaTourrette and Wasserburg 1998). Important constraints on the chronology of early solar system events and planetesimal size are provided by the evidence of retention or loss of decay products of the short-lived radio nuclides in the minerals from meteorites. Evidence of in situ decay of  $^{26}\text{Al}$ , which decays to  $^{26}\text{Mg}$  and has a half-life of 0.73 Myr (Walker et al. 1989), was documented in a number of studies of early-formed objects in the solar system (e.g., MacPherson et al. 1995). Specifically, it was found that plagioclase grains in many Ca- and Al-rich inclusions (CAIs), which constitute some of the earliest mineral phases in the solar system, have  $^{26}\text{Mg}$  excess

( $^{26}\text{Mg}^*$ ). Thus, LaTourrette and Wasserburg (1998) performed an experimental study of Mg diffusion in plagioclase and used the data to constrain the thermal history and, thereby, the size of planetesimals such that  $^{26}\text{Mg}$  was not completely lost from the plagioclase grains by diffusion. Following the suggestion of Urey (1955), they assumed that the planetesimals were heated by the heat generated from the decay of  $^{26}\text{Al}$ .

Besides  $^{26}\text{Mg}$ , another radiogenic product of short-lived radionuclide is  $^{41}\text{K}$  that formed from the decay of  $^{41}\text{Ca}$  in the early history of the solar system. The short half-life of  $^{41}\text{Ca}$  of 0.1 Myr makes the presence of radiogenic  $^{41}\text{K}$  a potentially useful indicator of the early solar system chronology. Excess  $^{41}\text{K}$  ( $^{41}\text{K}^*$ ), relative to the terrestrial abundance, was first demonstrated by Srinivasan et al. (1994) in the fassaite grains in the Efremovka, and suggested by Huneke et al. (1981) in fassaite and plagioclase

and by Hutcheon et al. (1984) in fassaite, melilite, and plagioclase in Allende. Sahijpal et al. (2000) demonstrated  $^{41}\text{K}^*$  in the fassaite and hibonite grains in Allende and in the hibonite grains in Murchison.  $^{41}\text{K}^*$  was also detected by Srinivasan et al. (1996) in two out of three melilite grains in the CAIs in Efremovka, while Ito et al. (2000) failed to find any evidence of  $^{41}\text{K}^*$  in three melilite grains in Allende that they examined. Although there are very limited data on  $^{41}\text{K}^*$  in melilite, the data above indicate that  $^{41}\text{K}^*$  in melilites in the CAIs were partly disturbed. Thus, additional constraints on the thermal history of the parent planetesimals of the CAIs could be obtained by deducing the condition at which  $^{41}\text{K}$  would be lost by diffusion from the melilites. In this work, we report the results of an experimental study of K diffusion in melilite, and apply these results to calculate the conditions under which  $^{41}\text{K}^*$  in melilite would be disturbed to different extents as a function of the accretion time scale and size of the parent planetesimals of CAIs.

## EXPERIMENTAL STUDIES

### Experimental Procedure

Melilite end-members, åkermanite ( $\text{Ca}_2\text{MgSi}_2\text{O}_7$ ) and gehlenite ( $\text{Ca}_2\text{Al}_2\text{SiO}_7$ ), were synthesized by the Czochralski-pulling method (Czochralski 1918) following the techniques described earlier by Yurimoto et al. (1989) and Morioka et al. (1997). Pure oxides of 3N quality, supplied by Wako Pure Chemical Co., were mixed in stoichiometric proportions, calcined at 1000 °C for several hours, and then loaded into an Ir crucible. The oxide mixture was heated to melting temperature and pulled vertically at a rate of 1 mm/hr using a seed crystal of melilite. The seed crystal was oriented previously by Laue back reflection and inserted into the top part of the melt so that its a-axis was vertical. As the melt was pulled, the seed crystal was rotated at a rate of 1–2 rotation(s) per minute. An earlier study by Morioka et al. (1997) confirmed that the synthetic melilite crystals grew with the a-axis parallel to the vertical direction of the furnace.

Since melilite is hexagonal, it is expected to have anisotropic diffusion properties with the principal diffusion axes coinciding with the a and c crystallographic directions. The diffusion coefficient  $D$  along any other direction must be intermediate between those along a- and c- directions and can be easily calculated from the latter values. We have, thus, cut the åkermanite and gehlenite crystals normal to the a-direction and, in addition, cut the gehlenite crystal normal to the c-direction to determine the anisotropy of K diffusion in this end-member. A cut slab was polished on one face in a stepwise manner down to the level of 0.25 µm diamond paste and finally finished, following Ganguly et al. (1998a), to a mirror polish by a combination of chemical and mechanical polishing using silica suspension on OP-chem cloth from

Struers (300 rpm). This final step ensures effective removal of a weak near-surface layer that might develop during mechanical polishing using diamond paste.

The oriented and polished samples were pre-annealed for 24 hr at 900 °C and 1 bar pressure to heal any line or planar defects that could have developed near the crystal surface during polishing and also to achieve a defect concentration close to those expected during diffusion experiments at 900–1100 °C. After this step, the polished surfaces of the samples were coated with a thin film of potassium by thermal evaporation of KOH under a high vacuum. The crystals were sealed in a silica tube and annealed for 1 hr to 10 days, depending on the temperature (Table 1), to induce measurable K diffusion profiles. Initially, we used KCl as the source of K, but after annealing the crystal surfaces showed small islands under an optical microscope of what appeared to be reacted areas. The measured diffusion profiles were also not reproducible. However, these problems disappeared when we used KOH as the source material for K.

### Measurement of Diffusion Profiles

The experimentally induced K diffusion profiles in the åkermanite and gehlenite crystals were measured by depth profiling of  $^{39}\text{K}$  in an ion microprobe (Cameca ims 3f SIMS at the Center for Solid State Science, Arizona State University), following the procedure described by Ganguly et al. (1998b). The primary ion beam was mass filtered negative  $^{16}\text{O}$  accelerated to 10 keV with a beam current of 20 to 80 nA. The beam spot size was ~30 to 60 µm in diameter. The samples were held at +4.5 kV resulting in an impact energy of 14.5 keV. The primary ion beam was rastered over  $\sim 125 \times 125$  µm square area during analyses. Electrostatic charging of a sample by the primary ion beam was virtually eliminated by a gold film of 40 nm thickness that was evaporated on the sample surface before the analyses.

Secondary ions were collected from the central domain of the rastered area using a mechanical aperture. This domain was of ~6 µm diameter. To eliminate interference by molecular ions, an offset of –75 V was applied to the sample voltage. The positive secondary ions of  $^{30}\text{Si}$ ,  $^{39}\text{K}$ ,  $^{42}\text{Ca}$ , and  $^{197}\text{Au}$  were monitored during the sputtering. Analyses of  $^{197}\text{Au}$ , which was deposited on the crystal surface to act as a thin conducting film, helped locate the crystal surface, while the concentration profiles of the non-diffusing species  $^{30}\text{Si}$  and  $^{42}\text{Ca}$  allowed us to monitor the stability of the analyses (Ganguly et al. 1998b). Plateau intensities of the non-diffusing species were achieved after a few measurement cycles, as seems to be typical for SIMS analyses. The data for  $^{39}\text{K}$  were ignored until the stabilization of the count rates for  $^{30}\text{Si}$  and  $^{42}\text{Ca}$  (Fig. 1). After a SIMS analysis, the flat-bottomed crater depth was determined with a TENCOR surface profilometer that was calibrated against known standards.

Table 1. Summary of experimental conditions and  $K$  diffusion coefficients in melilite. The errors represent approximately  $\pm 2\sigma$  values.

Mineral (diffusion direction)	Temp. (°C)	Time (hr)	$D$ (m <sup>2</sup> /s)	$\log D$ (m <sup>2</sup> /s)
<b>Åkermanite</b>				
(c)	900	167	$1.22 (\pm 0.18) \times 10^{-20}$	$-19.92 \pm 0.06$
(c)	950	96	$8.86 (\pm 1.49) \times 10^{-20}$	$-19.05 \pm 0.07$
(c)	1000	24	$2.26 (\pm 0.61) \times 10^{-19}$	$-18.65 \pm 0.12$
(c)	1000	48	$3.18 (\pm 0.50) \times 10^{-19}$	$-18.50 \pm 0.07$
(c)	1000	48	$1.60 (\pm 0.28) \times 10^{-19}$	$-18.80 \pm 0.07$
(c)	1050	24	$7.10 (\pm 0.80) \times 10^{-19}$	$-18.15 \pm 0.05$
(c)	1050	24	$4.40 (\pm 0.66) \times 10^{-19}$	$-18.36 \pm 0.06$
(c)	1077	12	$6.26 (\pm 0.96) \times 10^{-19}$	$-18.20 \pm 0.07$
(c)	1077	12	$7.83 (\pm 0.99) \times 10^{-19}$	$-18.11 \pm 0.06$
<b>Gehlenite</b>				
(c)	950	240	$2.79 (\pm 0.91) \times 10^{-21}$	$-20.55 \pm 0.14$
(c)	950	240	$2.89 (\pm 0.85) \times 10^{-21}$	$-20.54 \pm 0.13$
(c)	1000	10	$5.64 (\pm 1.49) \times 10^{-20}$	$-19.25 \pm 0.11$
(c)	1000	48	$3.60 (\pm 0.60) \times 10^{-20}$	$-19.44 \pm 0.07$
(c)	1000	48	$4.49 (\pm 0.63) \times 10^{-20}$	$-19.35 \pm 0.06$
(c)	1050	48	$7.43 (\pm 2.19) \times 10^{-20}$	$-19.13 \pm 0.13$
(c)	1084	12	$8.16 (\pm 1.74) \times 10^{-20}$	$-19.09 \pm 0.09$
(c)	1084	12	$7.12 (\pm 1.43) \times 10^{-20}$	$-19.15 \pm 0.09$
(c)	1200	1	$5.47 (\pm 1.10) \times 10^{-19}$	$-18.26 \pm 0.09$
(a)	900	168	$4.73 (\pm 0.58) \times 10^{-21}$	$-20.32 \pm 0.05$
(a)	1000	24	$3.41 (\pm 0.51) \times 10^{-20}$	$-19.47 \pm 0.06$
(a)	1000	24	$4.48 (\pm 0.43) \times 10^{-20}$	$-19.35 \pm 0.04$
(a)	1100	4	$4.28 (\pm 0.47) \times 10^{-19}$	$-18.37 \pm 0.05$
(a)	1100	4	$2.95 (\pm 0.28) \times 10^{-19}$	$-18.53 \pm 0.04$

### Modeling of Diffusion Profiles and Results

A typical diffusion profile of  $^{39}\text{K}$  parallel to the  $c$ -axis of gehlenite, and a model fit to the data, are shown in Fig. 1. The crystal surface ( $x = 0$ ) below the thin film was located on the basis of the intensity of  $^{197}\text{Au}$  signal, assuming that it was coincident with the depth profiling step where the intensity of this signal was reduced to half its peak value. Because of convolution effect,  $^{197}\text{Au}$  counts would not reduce to zero at the crystal surface, but instead would diminish smoothly to zero when the ion beam had penetrated inside the crystal. Data on semi-conducting materials for which the location of the interface could be independently established suggest that the interface is located approximately at the position where the  $^{197}\text{Au}$  counts are reduced to half the peak value (Hervig, personal communication). These strategies for the location of the interface and selection of  $^{39}\text{K}$  diffusion data are illustrated in Fig. 1.

The  $^{39}\text{K}$  diffusion data were modeled according to two different methods. In the first, the crystal surface was assumed to have a fixed concentration of the diffusing species (which implies that the source material was a semi-infinite homogeneous reservoir). In the second, the surface concentration of  $^{39}\text{K}$  was allowed to deplete with time

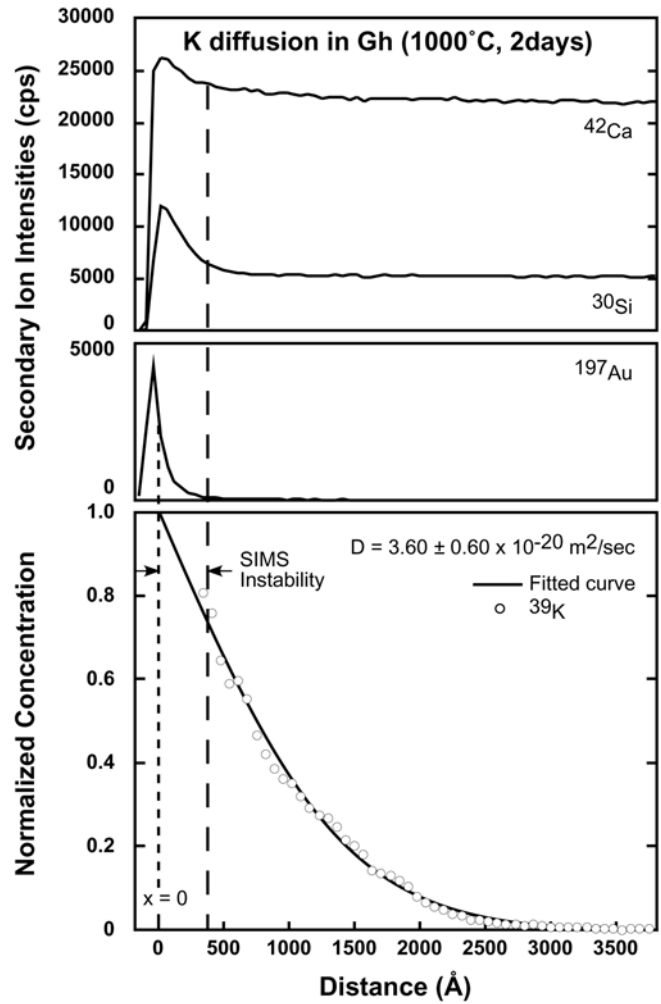


Fig. 1. Typical SIMS depth profile of  $^{39}\text{K}$  in gehlenite along with those of  $^{42}\text{Ca}$ ,  $^{30}\text{Si}$ , and  $^{197}\text{Au}$ . The crystal surface ( $x = 0$ ) was located to coincide with the depth at which the intensity of  $^{197}\text{Au}$  reduces to half the peak value, while the depth of simultaneous stabilization of  $^{42}\text{Ca}$ ,  $^{30}\text{Si}$  were used to determine the initial analytical cycles of instrumental instability. Only the  $^{39}\text{K}$  data after these initial unstable cycles were used for determining the diffusion coefficient. The model fit to the  $^{39}\text{K}$  data, according to the homogeneous infinite source model (Equation 1), is shown by solid line. The sample was diffusion-annealed for 2 days at 1 bar, 1000 °C, and the diffusion was parallel to  $c$ -axis.

(depleting source model). For these two models, the solutions of the diffusion equation with constant diffusion coefficient  $D$  are as follows (Crank 1975). For fixed surface concentration  $C_s$ :

$$\frac{C_s - C(x, t)}{C_s - C_\infty} = \text{erf}\left(\frac{x}{2\sqrt{Dt}}\right) \quad (1)$$

while for depleting surface concentration:

$$\frac{C(x, t) - C_\infty}{C_s - C_\infty} = K e^{-x^2/4Dt} \quad (2)$$

where  $x$  is the distance from the interface,  $t$  is the time, and  $C_\infty = C$  at  $t = 0, x$ . Since  $C_s$  could not be measured directly due to the initial instability of the ion beam (Fig. 1), we solved for both  $D$  and  $C_s$  by interfacing the above solutions to an optimization program, MINUIT, (James and Roos 1975). The latter yielded the combination of the values of  $C_s$  and  $D$  that best fit the experimental data. The fixed surface concentration model yielded a better fit to the experimental data than the depleted source model in all cases. The  $D$  values calculated from the former model are summarized, along with the experimental conditions, in Table 1. The statistical errors of  $D$  values were calculated numerically as follows. For a given profile, we calculated the  $D$  values for each point ( $C_i, x_i$ ) according to Equation 1, using the  $C_s$  value obtained from the optimization analysis. We then chose the domain around the mean that contains ~95% of the  $D$  values, and used it to define  $\sim 2\sigma$  error.

As is customary in the field of experimental diffusion studies, time series experiments were performed for both åkermanite and gehlenite crystals at 1000 °C to test if the experimental data were influenced by processes other than volume diffusion. Results of time series experiments, with 24 and 48 hr of annealing time for åkermanite and 10 and 48 hr for gehlenite, are summarized in Fig. 2. These data do not show any time dependence of the retrieved diffusion coefficients. However, as noted by Ganguly et al. (1998b), interference by other processes does not necessarily lead to time dependence of the retrieved (effective) diffusion coefficient.

Figure 3 shows the conventional Arrhenius plot,  $\log D$  versus  $1/T$ , of the experimental diffusion data of K in åkermanite and gehlenite. The parameters of the Arrhenius relation,  $D = D_0 e^{-E/RT}$ , where  $E$  is the activation energy of diffusion at 1 bar, were evaluated from the slopes and

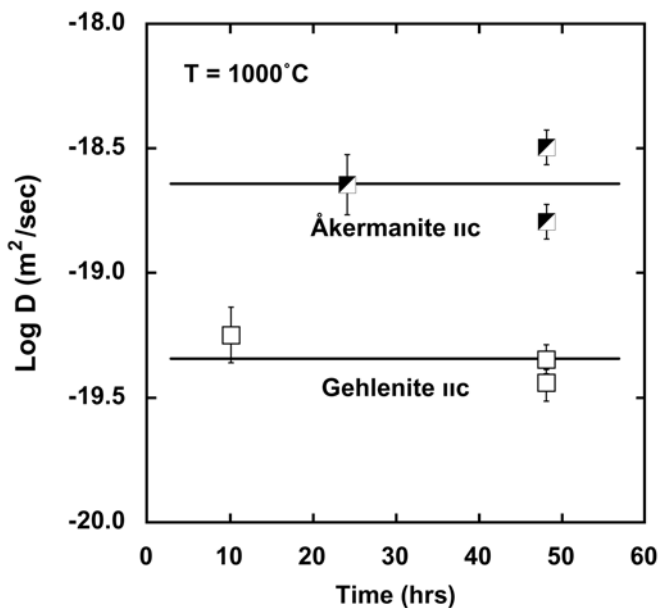


Fig. 2. Time series experiments of K diffusion ( $\parallel c$  axis) in åkermanite and gehlenite at 1 bar, 1000 °C.

intercepts of the regressed relations of  $\log D$  versus  $1/T$ , and are as follows ( $\pm 1\sigma$ ):

1. åkermanite ( $\parallel c$ ):  $\log D_0 = -7.6 \pm 1.1$  m<sup>2</sup>/s,  $E = 272 \pm 27$  kJ/mol;
2. gehlenite ( $\parallel c$ ):  $\log D_0 = -8.1 \pm 2.0$  m<sup>2</sup>/s,  $E = 284 \pm 49$  kJ/mol;
3. gehlenite ( $\parallel a$ ):  $\log D_0 = -7.4 \pm 0.7$  m<sup>2</sup>/s,  $E = 292 \pm 17$  kJ/mol.

The experimental results show that K diffusion in melilite is anisotropic with the  $D(\parallel c)$  around a factor of five greater than  $D(\parallel a)$ . Similar anisotropy of oxygen diffusion in melilite was also reported by Yurimoto et al. (1989). The diffusion coefficient along any arbitrary direction ( $\eta$ ) that has direction cosines of  $l$  and  $m$  with respect to the  $a$ - and  $c$ -axis, respectively, is given by (Crank 1975)  $D(\parallel \eta) = l^2 D(\parallel a) + m^2 D(\parallel c)$ .

## COSMOCHEMICAL IMPLICATIONS

### Closure Temperature of K in Melilites and Mg in Anorthite

We calculated the closure temperature  $T_c$  for the diffusive loss of  $^{41}\text{K}^*$  in melilite and  $^{26}\text{Mg}^*$  in anorthite from the modification of the classic Dodson formulation (Dodson 1973) by Ganguly and Tirone (1999). In its original form the Dodson formulation is not applicable to slowly diffusing species. The Ganguly-Tirone modification has removed this

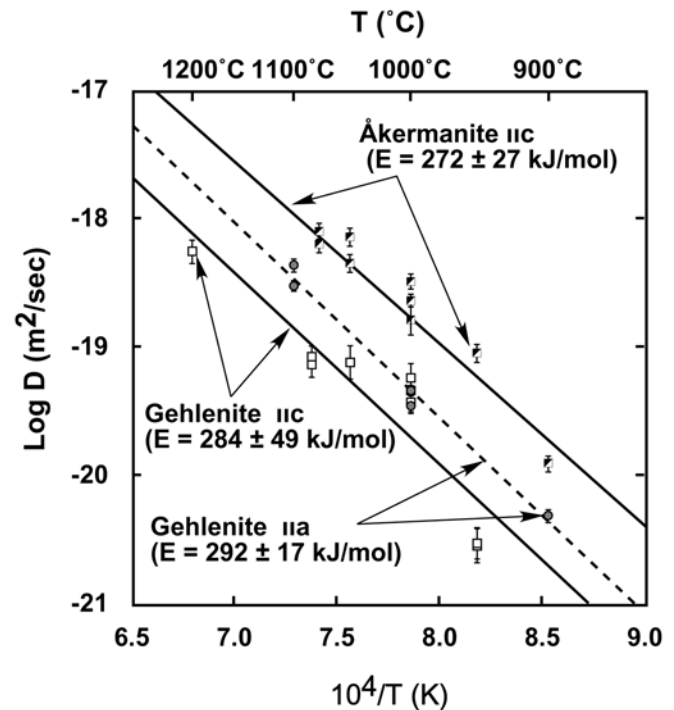


Fig. 3. Arrhenius plot of diffusion coefficient of  $^{39}\text{K}$  in åkermanite ( $\parallel c$  axis) and gehlenite ( $\parallel c, \parallel a$  axis). The solid lines are least squares fit to the experimental data that are shown as labeled symbols. The vertical bars on the symbols represent approximately  $\pm 2\sigma$  errors.

limitation of the Dodson formulation. The modified formulation is:

$$\frac{E}{RT_c} = \ln \left( \frac{A'RT_c^2 D_0}{E[dT/dt]a^2} \right) \quad (3)$$

where  $dT/dt$  is the cooling rate at  $T_c$ ,  $a$  is a characteristic dimension (radius for a sphere and cylinder, half-width for a plane sheet), and  $A' = e^{G+g}$ , where  $G$  is a geometric parameter with a fixed value for a specific crystal geometry (e.g., 3.29506 for a cylinder), and  $g$  is a function that depends on crystal shape, size, diffusion properties, and cooling rate (that is all parameters that affect  $T_c$ ). Equation 3 differs from the expression of  $T_c$  in the original Dodson formulation in the introduction of the term  $e^g$ . Without this term, the Dodson formulation may substantially overestimate  $T_c$  and may even lead to a solution of  $T_c$  that is higher than the initial temperature  $T_0$  when the diffusive loss is small (Ganguly and Tirone 2001).

Figure 4 shows calculated closure temperatures of K diffusion in åkermanite (Ak) and gehlenite (Gh) end-members and for a melilite of composition  $\text{Ak}_{20}\text{Gh}_{80}$ , along with that of anorthite, as function of cooling rate and grain size. The chosen melilite composition is typical for CAIs (Grossman 1975). The diffusion parameters for this intermediate composition were obtained by linear interpolation between those of the end-members. An order of magnitude change of the diffusion coefficient affects the  $T_c$  of K in melilite by  $\sim 10^\circ\text{C}$  for cooling rate of 10–100  $^\circ\text{C}/\text{Myr}$ . Thus, the estimated errors of the diffusion coefficient have insignificant effect on the calculation of  $T_c$ . Since melilite is hexagonal, we treated it as a cylinder. The melilites in CAIs are found to be typically  $\sim 1$  mm in radius, and 0.1 mm radius is probably at the lower limit of observed grain size of melilites in CAIs. The closure temperature of Mg in anorthite was calculated from the diffusion data of LaTourrette and Wasserburg (1998), and treating it as a plane sheet. The grain size (half-width) of anorthite in CAIs ranges up to 0.25 mm with an average of  $\sim 0.09$  mm (Simon, quoted in LaTourrette and Wasserburg 1998). The calculated closure temperature shows suggest that  $^{41}\text{K}^*$  in melilites should be disturbed to a lesser extent than  $^{26}\text{Mg}^*$ . However, as noted by Hutcheon (personal communication),  $^{41}\text{K}^*$  in melilite is extremely difficult to detect due to the low abundance of  $^{41}\text{Ca}$  and the relatively high concentration of K. Therefore, a careful search should be made in relatively K-depleted melilites.

#### Accretion Time and Size of Host Planetesimal

Using their Mg diffusion data in anorthite, LaTourrette and Wasserburg (1998) provided an important quantitative framework to constrain the size of planetesimals into which the CAIs were incorporated. They showed that if the CAIs were randomly distributed in the parent body that was heated

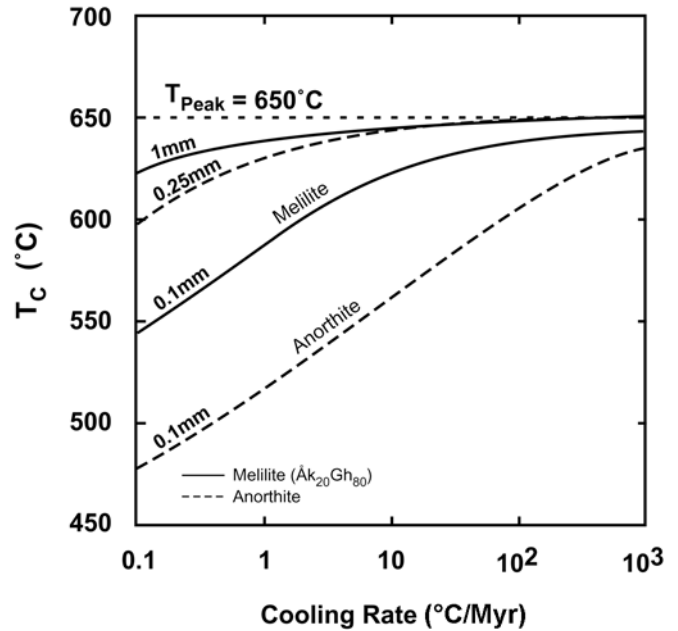


Fig. 4. Closure temperature  $T_c$  of K diffusion in melilite and Mg diffusion in anorthite as a function of cooling rate and grain size. The anorthite grain size in CAIs varies from an average of  $\sim 0.1$  mm to a maximum of 0.25 mm (half-width), while that of melilite varies from an average of  $\sim 1$  mm to a minimum of  $\sim 0.1$  mm radius.

by the decay of short-lived radioactive elements, then the grains buried below a critical planetesimal radius  $r_c$  would have almost completely lost  $^{26}\text{Mg}^*$  from anorthite. The value of  $r_c$  depends on the grain size of anorthite, and the radius  $R$  and formation time  $t_f$  of the planetesimal. Assuming that the heat needed to raise the temperature of the host planetesimal was completely derived by the decay of the short-lived  $^{26}\text{Al}$ , LaTourrette and Wasserburg (1998) calculated  $r_c/R$  as a function of  $R$  and  $t_f$ . Furthermore, they argued that since approximately 50% of CAIs show  $^{26}\text{Mg}^*$  in anorthite, the  $r_c$  should be such that it divides the planetesimal equally between an inner and outer volume segments, i.e.,  $(r_c/R)^3 = 0.5$  or  $r_c/R \sim 0.8$ .

Since fassaites in CAIs show  $^{41}\text{K}^*$ , the CAIs must have been incorporated in the planetesimals when significant quantity of  $^{41}\text{Ca}$  was still alive. Thus, the loss of  $^{41}\text{K}^*$  from the melilites (below the detection limit of an ion probe) must have taken place during the thermal evolution of the planetesimal. The thermal evolution models of planetesimals heated by  $^{26}\text{Al}$  decay, as calculated by LaTourrette and Wasserburg (1998), suggest that the cooling rates of the planetesimals were of the order of  $10^2$   $^\circ\text{C}/\text{Myr}$ . Thus, on the basis of the calculations of closure temperature of K diffusion in melilites as a function of cooling rate and grain size (Fig. 4), we conclude that in order for the melilite grains to lose  $^{41}\text{K}^*$  by diffusion, the host planetesimal must have been heated to a temperature of at least  $\sim 625^\circ\text{C}$ .

The thermal evolution of a spherical body of homogeneous initial temperature  $T_0$  and heated by the decay

of radioactive elements can be calculated from the solution heat diffusion equation with appropriate initial and boundary conditions. LaTourrette and Wasserburg (1998) assumed a fixed surface temperature  $T_o$  and internal heat production that decays with time according to  $A = A_o e^{-\lambda t}$ . An analytical solution for  $T(t, r)$  for this problem is given by Carslaw and Jaeger (1959). Instead of fixed surface temperature, Miyamoto et al. (1981) considered a linear radiation boundary condition:

$$\frac{dT}{dr} = -hT, \text{ when } r = R, t > 0 \quad (4)$$

and derived an analytical solution of the above heat diffusion problem with internal heat production from a single source. From a theoretical view point, the radiation boundary condition is more appropriate than a fixed surface temperature boundary condition for thermal evolution of a planetary body in the space. However, a body with a surface temperature  $T_s$  surrounded by a black body at a temperature  $T_o$  should be treated with the radiation boundary condition:

$$\left(\frac{dT}{dr}\right) = \frac{\sigma \varepsilon}{k} (T_s^4 - T_o^4), \text{ when } r = R, t > 0 \quad (5)$$

where  $\sigma$  is the Stefan-Boltzmann constant,  $\varepsilon$  is the emissivity of the surface and  $k$  is the thermal diffusivity (e.g., Özisik 1968). However, no analytical solution is available for the heat diffusion problem under this non-linear boundary condition. The problem was treated numerically by Ghosh and McSween (1998). In this work, we have linearized the radiation boundary condition, Equation 5, to the form of Equation 4, and used the analytical solution of Miyamoto et al. (1981). To linearize the boundary condition,  $dT/dr$  at the surface was calculated as a function of  $T_s$  for  $T_o = 100$ – $200$  K, using  $\varepsilon = 0.8$  (Miyamoto et al. 1981; Ghosh and McSween 1998). It was found that  $dT/dr$  remains essentially proportional to  $T_s$ , with  $h = -0.3147$  to  $-1.3885$  for  $T_o = 100$ – $200$  K, until  $T_s$  exceeds  $T_o$  by  $\sim 100$  K.

The solution to the heat diffusion equation for a spherical body with only one source term that produces heat according to the form  $A = A_o e^{-\lambda t}$  per unit volume, as derived by Miyamoto et al. (1981), is as follows:

$$T = T_o + \frac{2hR^2 A}{rK} \sum_{n=1}^{\infty} \frac{1}{1 - \lambda/k\alpha_n^2} \cdot \frac{(\exp[-\lambda t] - \exp[-k\alpha_n^2]) \sin(r\alpha_n)}{\alpha_n^2 (R^2 \alpha_n^2 + R \cdot h[R \cdot h - 1]) \sin(R\alpha_n)} \quad (6)$$

where  $T_o$  is the initial temperature,  $\alpha_n$  is the  $n$ -th root of the equation  $(R\alpha)\cot(R\alpha) + Rh - 1 = 0$ ,  $K$  is the thermal conductivity,  $k$  is the thermal diffusivity,  $\rho$  is the density,  $\lambda$  is the decay constant of the heat producing radionuclide,  $r$  is the

radial distance from the center, and  $R$  is the radius of the parent body. Calculation of  $T_s$  using Equation 6 and the above values of  $h$  show very little change of  $T_s$  as function of time. Thus, not only could the boundary condition be linearized without introducing any significant error, but also there should be very little difference between the results of thermal evolution of a planetary body obtained from using constant surface temperature and radiation boundary conditions. In this work, we have used the linearized radiation boundary condition.

The primary cause of heating of a planetesimal is the decay of  $^{26}\text{Al}$  (Urey 1955) and to a lesser extent that of  $^{60}\text{Fe}$  (Shukolyukov and Lugmair 1993). It can be easily shown that if there is an additional heat source (radionuclide) that produces heat according to the same exponential form as above, then one simply needs to add an additional term to the solution of  $T(r, t)$  in the same form as for the first radionuclide. The initial heat production rate at the time of planetesimal formation,  $t_f$ , is essentially constrained by the amount of these short-lived radioactive elements that were still extant at that time. Using a canonical solar system value of  $^{26}\text{Al}/^{27}\text{Al}$  of  $5 \times 10^{-5}$ , the specific heat production rate,  $H_o(t_f)$ , due to the decay of  $^{26}\text{Al}$  at  $t_f$  was calculated by LaTourrette and Wasserburg (1998) to be  $(2.7 \times 10^{-7}) \exp(-\lambda_{\text{Al}} t_f)$  W/kg, where  $\lambda_{\text{Al}}$  is the decay constant of  $^{26}\text{Al}$ . Birck and Lugmair (1988) estimated  $^{60}\text{Fe}/^{56}\text{Fe}$  ratio of  $1.6 \times 10^{-6}$  in Allende CAI, while Tachibana and Huss (2003) suggested a lower initial solar system  $^{60}\text{Fe}/^{56}\text{Fe}$  ratio of  $\sim 3 \times 10^{-7}$ . These data yield  $H_o(t_f) = H^* \exp(-\lambda_{\text{Fe}} t_f)$ , where  $\lambda_{\text{Fe}}$  is the decay constant of Fe, with  $H^*$  of  $1.97 \times 10^{-8}$  and  $3.7 \times 10^{-9}$  W/kg according to the data of Birck and Lugmair (1988) and Tachibana and Huss (2003), respectively. In these calculations of  $H^*$ , we have used heat production due to the decay of  $^{60}\text{Fe}$  to be 2.78 MeV/atom (Lederer and Shirley 1978) and the total Fe content to be 19 wt% in CI chondrite (Anders and Grevesse 1989).

Figure 5 illustrates the results of our calculation of the thermal evolution of a planetesimal as a function of  $t_f$ ,  $r_c/R$  and  $R$ , using both  $^{26}\text{Al}$  and  $^{60}\text{Fe}$  as the heat sources, and assuming initial temperature  $T_o$  of 100 and 200 K. LaTourrette and Wasserburg (1998) assumed  $T_o = 100$  K, while Bennett and McSween (1996) argued that  $T_o$  could not have been less than 160 K. In the calculations in Fig. 5, we assumed that the planetesimal had achieved a peak temperature of 625 °C at a specified value of  $r_c/R$ . This is approximately the minimum temperature needed for any significant disturbance of  $^{41}\text{K}^*$  in melilite, according to the calculation of closure temperature (Fig. 4), in typical melilite grains in the CAIs that are  $\sim 1$  mm in radius. With the peak temperature fixed to a specific value, the value of  $R$  depends on the combination of values of  $t_f$  and  $r_c/R$ . For specified values of  $t_f$  and  $r_c/R$ , the estimate of initial  $^{60}\text{Fe}/^{56}\text{Fe}$  ratio by Tachibana and Huss (2003) yields a larger value of  $R$  compared to that derived from the estimate of the initial ratio by Birck and Lugmair (1984), when  $t_f > 2$  Myr.

The planetesimal radius that is needed to disturb a specific

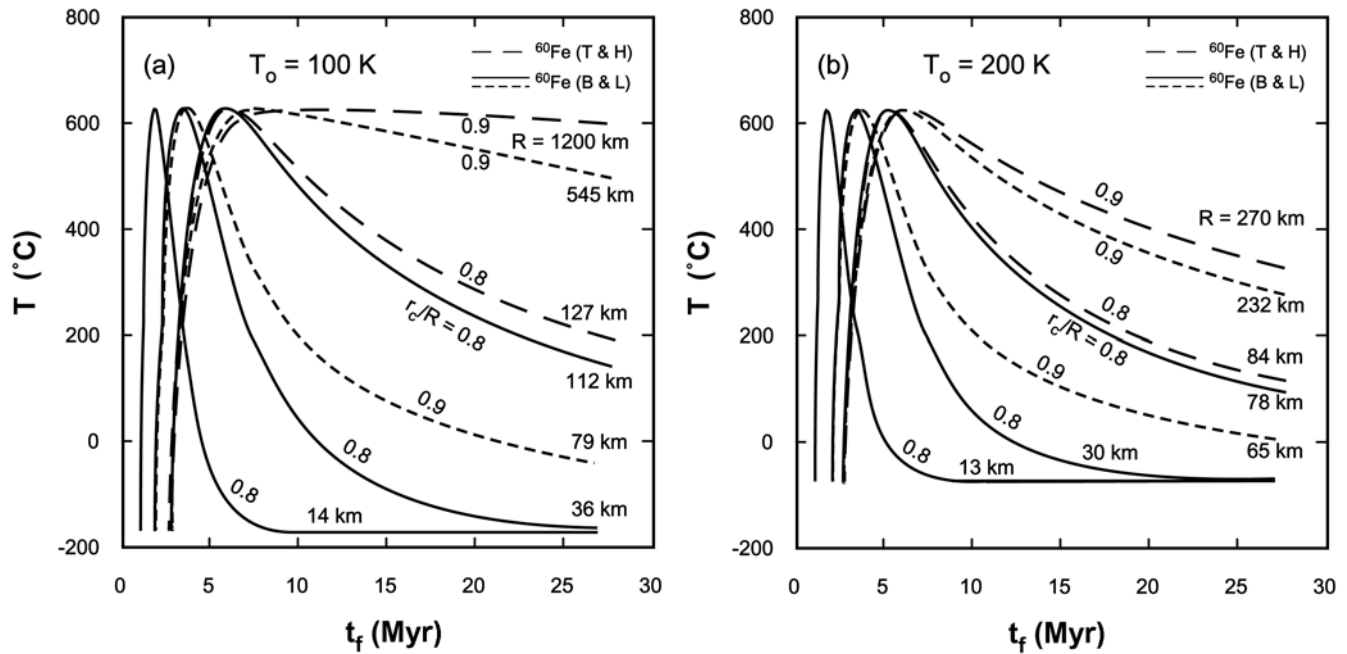


Fig. 5. Thermal evolution of planetesimals, assumed to be spherical bodies and heated by the decay of  $^{26}\text{Al}$  and  $^{60}\text{Fe}$ , as a function of accretion time  $t_f$ , radius  $R$ , and the ratio of critical radial distance  $r_c$  to  $R$  (shown as numbers on the curves) that experienced peak temperature of 625 °C. The initial temperature  $T_o$  of the planetesimal was assumed to be: a) 100 K and b) 200 K. The solid and short dashed lines were calculated on the basis of  $^{60}\text{Fe}/^{56}\text{Fe}$  solar initial ratio estimated by Birck and Lugmair (1998), while the long dashed lines were calculated on the basis of the initial ratio due to Tachibana and Huss (2003).

percentage of randomly distributed melilite grains is shown in Figs. 6a–6d as a function of  $t_f$  using  $T_o$  of 100 and 200 K. Assuming random distribution of CAIs within a planetesimal, the fraction of melilite grains disturbed equals the fraction of the planetesimal volume (i.e.,  $[r_c/R]^3$ ) that experienced temperature at or above 625 °C, the latter being the temperature at  $r_c$ . Also shown for comparison are the data for significant retention of  $^{26}\text{Mg}^*$  in ~50% of anorthite grains, using  $^{26}\text{Al} + ^{60}\text{Fe}$  as the heat source (dashed lines in the main body). Here, we used the condition, following LaTourrette and Wasserburg (1998), that the  $\int D(t)dt$  over the calculated  $T$ - $t$  path at  $r_c$ , equals  $0.25a^2$ , where  $a$  is the radius or half-width of a grain. This procedure satisfies the condition of 90% loss  $^{26}\text{Mg}^*$  from a plagioclase grain by diffusion at the  $T$ - $t$  condition at  $r_c$  (a higher value of this integral,  $\sim 0.4a^2$ , seems more appropriate for 90% loss, according to the results in Crank [1975], but changing the value of the integral from  $0.25a^2$  to  $0.4a^2$  has an insignificant effect on the calculated value of  $R$ ). The results for  $T_o = 100$  K with  $^{26}\text{Al}$  as the only heat source were calculated earlier by LaTourrette and Wasserburg (1998).

The inset of Fig. 6a shows the effect of including  $^{60}\text{Fe}$  as a heat source in addition to  $^{26}\text{Al}$ . The curves refer to the condition for the disturbance of  $^{26}\text{Mg}^*$  in 50% anorthite grains. It is evident from these results that  $^{60}\text{Fe}$  has significant effect on the thermal budget of a planetesimal if one accepts the estimate of initial solar ratio of  $^{60}\text{Fe}/^{56}\text{Fe}$  by Birck and Lugmair (1988), but it has only minor effect according to the more recent estimate of the initial ratio by Tachibana and

Huss (2003). Figures 6a (main body) and 6c illustrate the  $R$  versus  $t_f$  relations using the initial  $^{60}\text{Fe}/^{56}\text{Fe}$  ratio by the latter group, while Figs. 6b and 6d illustrate the same relations using the initial  $^{60}\text{Fe}/^{56}\text{Fe}$  by the former group.

The calculations presented in Fig. 6 show that if  $^{26}\text{Mg}^*$  was essentially lost from ~50% of the anorthite grains, then we should expect disturbance of  $^{41}\text{K}^*$  in ~40% of melilite grains. On the other hand, if  $^{41}\text{K}^*$  in the majority of melilite grains were disturbed, then the required planetesimal size would have to be larger than that needed to at least partially retain  $^{26}\text{Mg}^*$  in 50% of the anorthite grains. Invoking a short-lived partial melting event would not alleviate the problem that would be created if  $^{41}\text{K}^*$  were disturbed in the majority of melilite grains, since the melting temperature of melilite (1400 °C) is much higher than that of either anorthite (1250 °C) or clinopyroxene (1225 °C) (Stolper 1982). Consequently, both anorthite and fassaite would have completely lost  $^{26}\text{Mg}^*$  and  $^{41}\text{K}^*$ , respectively, if the melilites were to lose  $^{41}\text{K}^*$  by melting.

On the basis of the  $^{26}\text{Al}/^{27}\text{Al}$  ratio in chondrules, Kita et al. (2000) and Kunihiro et al. (2004) estimated the time of chondrule formation to be 2 Myr and 2.7 Myr, respectively. In view of the very rapid cooling rate that seems to be required for the chondrule formation (Lofgren 1994), we assume that the chondrules formed before the accretion of the planetesimals. Thus, if we set the chondrule formation time as a minimum limit of the planetesimal accretion time, then the calculations in Fig. 6 suggest a minimum

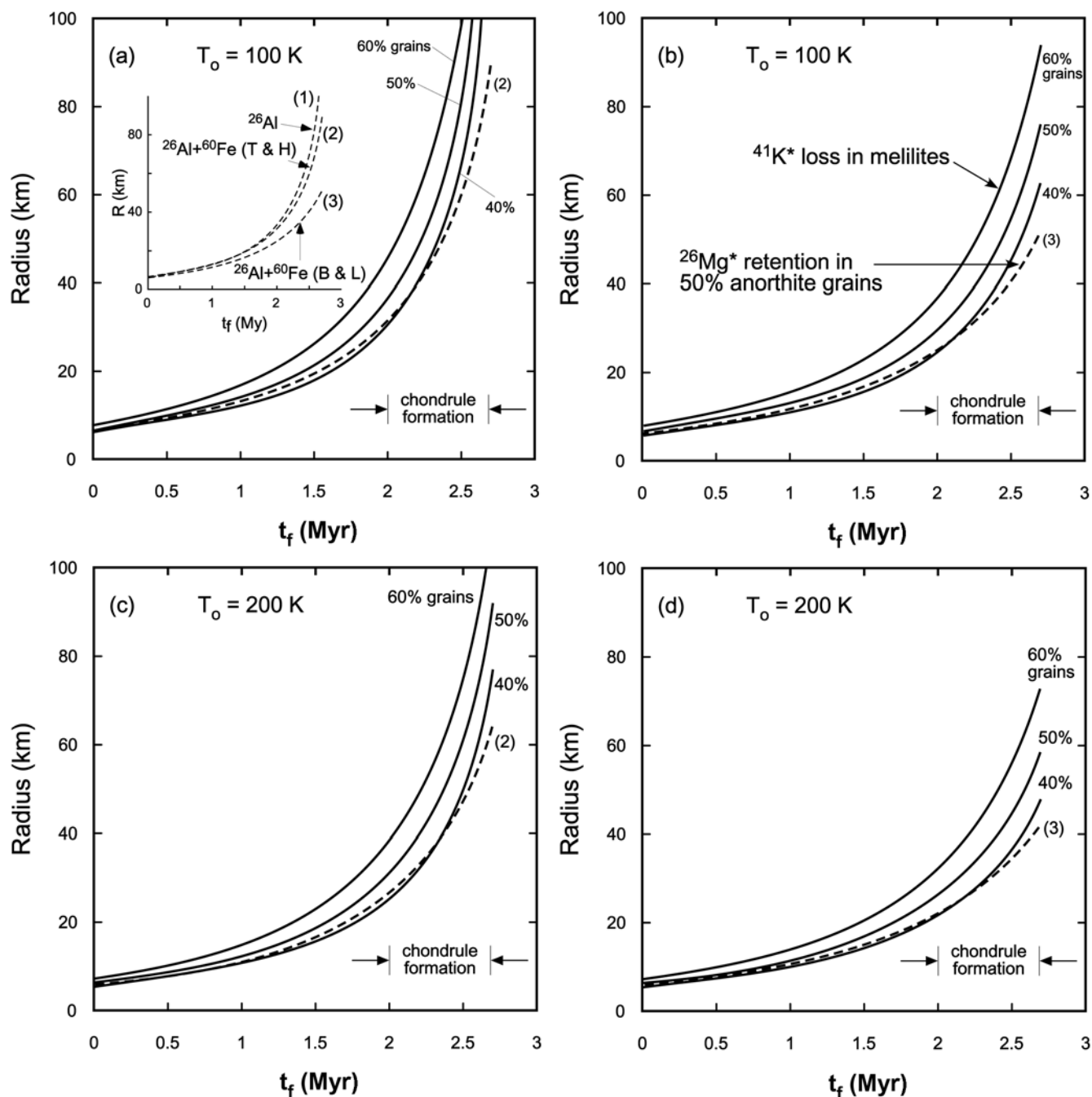


Fig. 6. Radius of planetesimal as a function of the accretion time  $t_f$  and percentages of melilite and anorthite grains with disturbed isotopic systems, using both  $^{26}\text{Al}$  and  $^{60}\text{Fe}$  as the heat source. It is assumed that 50% of anorthite grains almost completely lost  $^{26}\text{Mg}^*$  (dashed line), while the indicated percentages of the melilite grains were heated at least up to the closure temperature (625 °C) of K diffusion in melilites. The inset in (a) shows the effect of incorporation of  $^{60}\text{Fe}$  as a heat source with the solar initial  $^{60}\text{Fe}/^{56}\text{Fe}$  ratio estimated by Birck and Lugmair (B & L) and Tachibana and Huss (T & H). The initial temperature  $T_0$  was assumed to be: a, b) 100 K and c, d) 200 K. In (a) and (c)  $^{60}\text{Fe}/^{56}\text{Fe}$  solar initial ratio according to Tachibana and Huss (2003); in (b) and (d)  $^{60}\text{Fe}/^{56}\text{Fe}$  solar initial ratio according to Birck and Lugmair (1988).

planetesimal radius of ~20–30 km if  $^{26}\text{Mg}^*$  were almost completely lost from ~50% of anorthite grains, as suggested by LaTourette and Wasserburg (1998), and there was a compatible disturbance of  $^{41}\text{K}^*$  in ~40% melilite grains. On the other hand, if  $^{41}\text{K}^*$  were disturbed in significantly more melilite grains, then the planetesimal radius would have to

be larger than that permitted by the criterion that  $^{26}\text{Mg}^*$  was disturbed in ~50% anorthite grains. However, it is unclear at this stage how stringent the latter criterion is, since the type B CAIs that have been so extensively analyzed for Al-Mg systematics are only found in CV chondrites (A. Davis, personal communication).



**Acknowledgments**—This research was supported by NASA grants NAG5-7364 and NNG04GG26G, and a post-doctoral fellowship for research abroad to the senior author from the Japan Society for the Promotion of Sciences. Thanks are due to Dr. Rick Hervig for access to his ion-probe laboratory and advice. M. Ito would like to thank Dr. Takuya Kunihiro for discussion, and Dr. Masana Morioka for his help in synthesizing åkermanite and gehlenite crystals at the Radioisotope Center, University of Tokyo. The paper has greatly benefited from the constructive reviews of Dr. Ian Hutcheon and Dr. Andrew Davis, and the careful editorial handling and helpful suggestions of Dr. Kevin Righter.

**Editorial Handling**—Dr. Kevin Righter

## REFERENCES

- Anders E. and Grevesse N. 1989. Abundances of the elements: Meteoritic and solar. *Geochimica et Cosmochimica Acta* 53:197–214.
- Bennett M., III, and McSween H. Y., Jr. 1996. Revised model calculations for the thermal histories of ordinary chondrite parent body. *Meteoritics & Planetary Science* 31:783–792.
- Birck J. L. and Lugmair G. W. 1988. Nickel and chromium isotopes in Allende inclusions. *Earth and Planetary Science Letters* 90:131–143.
- Carslaw H. S., and Jaeger J. C. 1986. *Conduction of heat in solids*, 2nd ed. Oxford: Oxford University Press. 510 p.
- Crank J. 1975. *The mathematics of diffusion*, 2nd ed. Oxford: Oxford University Press. 424 p.
- Czochralski J. 1918. Ein neues Verfahren zur Messung der Kristallisationsgeschwindigkeit der Metalle. *Zeitschrift für Physikalische Chemie* 92:219–221.
- Dodson M. H. 1973. Closure temperature in cooling geochronological and petrological systems. *Contributions to Mineralogy and Petrology* 40:259–274.
- Ganguly J., Cheng W., and Chakraborty S. 1998a. Cation diffusion in aluminosilicate garnets: Experimental determination in pyroxene-almandine diffusion couples. *Contributions to Mineralogy and Petrology* 131:171–180.
- Ganguly J., Tirone M., and Hervig R. L. 1998b. Diffusion kinetics of samarium and neodymium in garnet, and a method for determining cooling rates of rocks. *Science* 281:805–807.
- Ganguly J. and Tirone M. 1999. Diffusion closure temperature and age of a mineral with arbitrary extent of diffusion: Theoretical formulation and applications. *Earth and Planetary Science Letters* 170:131–140.
- Ganguly J. and Tirone M. 2001. Relationship between cooling rate and cooling age of a mineral: Theory and application to meteorites. *Meteoritics & Planetary Science* 36:167–175.
- Ghosh A. and McSween H. Y., Jr. 1998. A thermal model for the differentiation of asteroid 4 Vesta based on radiogenic heating. *Icarus* 134:187–206.
- Grossman L. 1975. Petrography and mineral chemistry of Ca-rich inclusions in the Allende meteorite. *Geochimica et Cosmochimica Acta* 39:433–454.
- Huneke J. C., Armstrong J. T., and Wasserburg G. J. 1981.  $^{41}\text{K}$  and  $^{26}\text{Mg}$  in Allende inclusions and a hint of  $^{41}\text{Ca}$  in the early solar system (abstract). 12th Lunar and Planetary Science Conference. pp. 482–484.
- Hutcheon I. D., Armstrong J. T., and Wasserburg G. J. 1984. Excess  $^{41}\text{K}$  in Allende CAI: Confirmation of a hint (abstract). 15th Lunar and Planetary Science. pp. 387–388.
- Ito M., Yurimoto H., and Nagasawa H. 2000. A study of Mg and K isotopes in Allende CAIs: Implication to the time scale for the multiple heating processes (abstract #1600). 31st Lunar and Planetary Science Conference. CD-ROM.
- James F. and Roos M. 1975. MINUIT: A system for function minimization and analysis of the parameter errors and correlations. *Computer Physics Communications* 10:343–367.
- Kita N. T., Nagahara H., Togashi S., and Morishita Y. 2000. A short duration of chondrule formation in the solar nebula: Evidence from  $^{26}\text{Al}$  in Semarkona ferromagnesian chondrules. *Geochimica et Cosmochimica Acta* 64:3913–3922.
- Kunihiro T., Rubin A. E., McKeegan K. D., and Wasson J. T. 2004. Initial  $^{26}\text{Al}/^{27}\text{Al}$  in carbonaceous-chondrite chondrules: Too little  $^{26}\text{Al}$  to melt asteroids. *Geochimica et Cosmochimica Acta* 68:2947–2957.
- LaTourrette L. and Wasserburg G. J. 1998. Mg diffusion in anorthite: Implications for the formation of early solar system planetesimals. *Earth and Planetary Science Letters* 158:91–108.
- Lederer C. M. and Shirley V. S., eds. 1978. *Table of isotopes*, 7th ed. New York: Wiley-Interscience. 1628 p.
- Lofgren G. E. 1994. Experimental constraints on models for the origin of chondrules: Cooling rates (abstract). Proceedings, Workshop on Chondrules and the Protoplanetary Disk. LPI contribution #844. Houston: Lunar and Planetary Institute. pp. 19–20.
- MacPherson G. J., Davis A. M., and Zinner E. K. 1995. The distribution of aluminum-26 in the early solar system: A reappraisal. *Meteoritics* 30:365–377.
- Miyamoto M., Fujii N., and Takeda H. 1981. Ordinary chondrite parent body: An internal heating model. Proceedings, 12th Lunar and Planetary Science Conference. pp. 1145–1152.
- Morioka M., Kamata Y., and Nagasawa H. 1997. Diffusion in single crystal of melilite: III. Divalent cations in gehlenite. *Geochimica et Cosmochimica Acta* 61:1009–1016.
- Özişik M. N. 1968. *Boundary value problems of heat conduction*. Scranton: International Textbook Co. 505 p.
- Sahijpal S., Goswami J. N., and Davis A. M. 2000. K, Mg, Ti, and Ca isotopic compositions and refractory trace element abundances in hibonite from CM and CV meteorites: Implications for early solar system processes. *Geochimica et Cosmochimica Acta* 64:1989–2005.
- Shukolyukov A. and Lugmair G. W. 1993. Live iron-60 in the early solar system. *Science* 259:1138–1142.
- Srinivasan G., Ulyanov A. A., and Goswami J. N. 1994.  $^{41}\text{Ca}$  in the early solar system. *The Astrophysical Journal* 431:L67–L70.
- Srinivasan G., Sahijpal S., Ulyanov A. A., and Goswami J. N. 1996. Ion microprobe studies of Efremovka CAIs: II. Potassium isotope composition and  $^{41}\text{Ca}$  in the early solar system. *Geochimica et Cosmochimica Acta* 60:1823–1835.
- Stolper E. 1982. Crystallization sequences of Ca-Al-rich inclusions from Allende: An experimental study. *Geochimica et Cosmochimica Acta* 46:2159–2180.
- Tachibana S. and Huss G. R. 2003. The initial abundance of  $^{60}\text{Fe}$  in the solar system. *The Astrophysical Journal* 588:L41–L44.
- Urey H. C. 1955. The cosmic abundances of potassium, uranium, and thorium and the heat balances of the Earth, the Moon, and Mars. *Proceedings of the National Academy of Sciences* 41:127–144.
- Yurimoto H., Morioka M., and Nagasawa H. 1989. Diffusion in single crystal of melilite: I. Oxygen. *Geochimica et Cosmochimica Acta* 60:1823–1835.
- Walker F. W., Parrington J. R., and Feiner F. 1989. *Nuclides and isotopes. Chart of the nuclides*, 14th ed. San Jose: GE Nuclear Energy/GE Electric Company. 57 p.